Research Article | Vol. 27, No. 12 | 10 Jun 2019 | OPTICS EXPRESS 17112

Optics EXPRESS

Two-wavelength Tm:YLF/KGW external-cavity Raman laser at 2197 nm and 2263 nm

UZZIEL SHEINTOP,[1,2] DANIEL SEBBAG,[1] PAVEL KOMM,[2] SHAUL PEARL,[3] GILAD MARCUS,[2] AND SALMAN NOACH[1,*]

[1]*Department of Applied Physics, Electro-optics Engineering Faculty, Jerusalem College of Technology, Hava'ad Haleumi 21, Jerusalem, Israel*
[2]*Department of Applied Physics, Faculty of Mathematics & Sciences, The Hebrew University of Jerusalem, Jerusalem, Israel*
[3]*Applied Physics Division, Soreq Nuclear Research Center, Yavne 81800, Israel*
[*]*salman@jct.ac.il*

Abstract: This paper presents a KGW Raman laser with an external-cavity configuration at the 2 µm region. The Raman laser is pumped by an actively Q-switched Tm:YLF laser, especially designed for this purpose emitting at 1880 nm. Due to the KGW bi-axial properties, the Raman laser is able to lase separately at two different output lines, 2197 nm and 2263 nm. The output energies and pulse durations that were achieved for these two lines are 0.15 mJ/pulse at 21 ns and 0.4 mJ/pulse at 5.4 ns, respectively. To the best of our knowledge, this is the first time that the KGW crystal, which is well known for its wide use in shorter wavelengths, is demonstrated in a Raman laser in the 2 µm region. According to the achieved results and due to the KGW properties, it appears to be a suitable crystal for energy scaling and efficient Raman conversion in this spectral range. An estimation of the Raman gain coefficient for this wavelength is provided as well.

1. Introduction

In the past few years, there has been a growing demand for high-power lasers emitting at wavelength beyond 2 µm. Lasers at these "retina-safe" wavelengths have several potential applications, including LIDAR, biomedicine [1], polymer material processing [2], defense applications, and gas sensing [3]. Therefore, 2 µm (SWIR) coherent sources have drawn much attention, as is evident from the recent efforts to develop high power lasers that cover this spectral range [3-5].

Within this context, solid-state Raman lasers lend themselves to an interesting approach. They are efficient and useful high-brightness sources that extend the spectral span of existing lasers and fill the spectral gaps between them [6-9]. Compared to OPO, Raman lasers have advantages such as narrow linewidth, avoid of phase matching constraints, pulse length shortening and beam quality improvement through Raman beam cleanup [10]. However, solid-state Raman lasers are mostly implemented in the visible and ~1 µm regions and only rarely in the SWIR region. The reasons for this are two fold, first because the stimulated-Raman-scattering (SRS) gain coefficient drops theoretically approximately according to inverse wavelength, resulting in lower efficiency compared to NIR Raman lasers [6]. The second reason is the lack of suitable high power pump lasers that have sufficient gain over the Raman stimulated threshold. Recent developments in high-power pulsed Tm-doped and Ho-doped solid-state lasers in the 2 µm region [5,11-14] expands the availability of pump sources that can be used for efficient Raman laser conversion in this spectral range. Those lasers can be designed to have high peak power, linear polarization and narrow bandwidth, characteristics which are often required to match the Raman gain properties [6, 8, 15, 16].

The first demonstrations of SRS conversion in 2 µm using Tm:$KY(WO_4)_2$ and $BaWO_4$ crystals were reported more than a decade ago [17, 18]. However, these reports lack

#357739 https://doi.org/10.1364/OE.27.017112
Journal © 2019 Received 8 Feb 2019; revised 4 Apr 2019; accepted 5 Apr 2019; published 4 Jun 2019

information about the obtained output energy. Since 2013, several studies have demonstrated crystalline Raman lasers in the 2 to 4 μm region: A $BaWO_4$ crystal pumped by a Tm:YAP laser emitting at 2360 nm achieved 0.31 mJ of output energy [19], a YVO_4 crystal pumped by a Tm:YAP laser emitting at 2418 nm yielded 0.27 mJ of output energy [20], a $BaWO_4$ crystal pumped by a Tm,Ho:$GdVO_4$ laser emitting at 2533 nm obtained 0.31 mJ of output energy [21, 22], a $BaWO_4$ crystal pumped by a Ho:YAG laser emitting at 2602 nm yielded 0.27 mJ of output energy [23], and a diamond crystal pumped by a tunable OPO around 2.4 μm, emitting from 3.38 to 3.80 μm attained up to 0.12 mJ of output energy [24]. The highest conversion efficiency of these lasers was 13.9% (6.8% efficiency from pump diode, for intracavity lasers).

Except for the Ho:YAG/ $BaWO_4$ and diamond laser [23,24], all these solid-state Raman lasers were implemented using an intracavity configuration, where the Raman medium is placed within the fundamental laser cavity, thus utilizing all the energy which exists inside the cavity. The external cavity configuration, in which the Raman cavity is separated from the fundamental laser, is more reliable from design considerations and alignment constraints. It facilitates the control of the pump power density in the Raman crystal, by proper design of the delivering optics between the fundamental and Raman lasers. In addition, with this architecture, it is easier to achieve mode matching and proper thermal management, since the two cavities are separated.

The aforementioned works investigated 2 μm Raman lasing by using mainly $BaWO_4$. Since it is possible to obtain SRS in a wide selection of Raman crystals, one should search for other Raman media with good conversion efficiency in the 2 μm. In this context, one of the most popular tungstate Raman crystals is potassium gadolinium tungstate ($KGd(WO_4)_2$ or KGW) owing to its good optical and thermal properties. The KGW has high damage threshold and its negative thermo-optic coefficient mitigates the onset of thermal lensing compared to other Raman crystals [6, 25]. Moreover, because KGW is biaxial, it has Raman interaction with two different vibrational modes (901 cm^{-1} and 768 cm^{-1}), yielding the option to obtain two different Stokes wavelengths by controlling the polarization of the pump [25]. To date, KGW has been used in the visible and 1 μm segment only and numerous reviews are available on the performance of this medium when pumped near 1 μm and shorter [6-9]. Approaching longer wavelengths in the 2 μm region using a KGW crystal is challenging because of the theoretically abovementioned dependence of the Raman gain coefficient on the wavelength. Based on experimental results presented in this paper, an estimation of the gain coefficient for the KGW at the 2 μm is provided for the first time.

In this paper we present an external-cavity KGW Raman laser, pumped by an actively Q-switched Tm:YLF laser which operates at 1880 nm with 1 kHz repetition rate. This Raman laser can operate at two different wavelengths. At the first operating wavelength of 2197 nm, we obtained an output energy of 0.15 mJ/pulse and a 5.4 ns pulse duration. At the second wavelength of 2263 nm, a higher energy of 0.4 mJ/pulse was reached; however, a longer pulse duration of 21 ns was measured. To the best of our knowledge, this is the first Raman laser in the 2 μm region based on a KGW crystal as an active gain medium. The use of KGW allows to achieve the highest pulse energy reported in this spectral region. Part of this work was presented at the ASSL conference in 2018 [26].

2. Experimental setup

The experimental setup of the Raman laser and its fundamental pump source is shown in Fig. 1. The fundamental laser is an actively Q-switched Tm:YLF laser with an end-pumped architecture. This laser was described in detail in a previous study [27]. Briefly, a 9 mm length Tm:YLF (3.5% at.) with a 3 × 3 mm^2 cross-section, pumped by a 793 nm laser-diode, is used as a gain medium. Both the diode and Tm:YLF crystal are water-cooled to 19°C. The input mirror of the Tm:YLF cavity is a flat mirror that is coated for high transmission (HT) at 793 nm and high reflectivity (HR) around 1900 nm. An output-coupler (OC) with a 200 mm radius of curvature (ROC) that is coated for a partial reflection (PR) of 70% around 1900 nm is placed 200 mm from the input mirror. A water-cooled (19°C) acousto-optic-modulator (AOM), with an AO medium made of 45 mm long fused silica, is used as an active Q-switch. Two uncoated yttrium aluminum garnet (YAG) etalon plates, with 500 µm and 25 µm thicknesses, are inserted into the laser cavity to narrow the laser spectral line. When pumped by a maximum power of 15.6 W at 793 nm, an average power of 2.35 W is obtained at 1 kHz. The lasing wavelength is measured to be 1880 nm with a spectral width of ~0.15 nm with the etalon pair, whereas without them, the spectral width was ~1.4 nm. The pulse duration was measured to be 34 ns full width at half-maximum (FWHM). The laser beam is linearly p-polarized.

The output emission from the Tm:YLF is imaged by a pair of antireflective (AR) coated, biconvex lenses, to a spot diameter of ~220 µm in the center of the KGW crystal. Due to divergence of the beam, the beam size increases to 300 µm at the facets of the Raman crystal.

A half-wave-plate (HWP) was added between the lenses to control the polarization orientation and enable switching between the two different Raman vibration shifts of the KGW crystal, thus enabling selective lasing at 2197 nm and 2263 nm. Such an external cavity configuration is advantageous for a two-wavelength Raman laser, since it allows for easy switching between the two Raman-shifted modes. Owing to losses from the optical delivery components from the fundamental laser to the Raman laser, the available maximal pump energy for the Raman laser is 1.99 mJ/pulse.

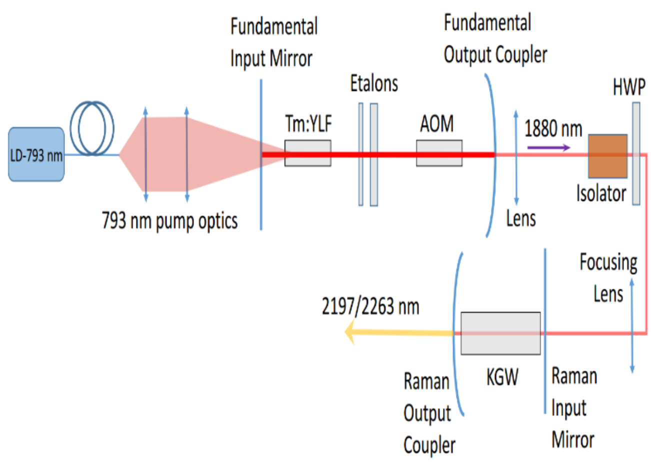

Fig. 1. Schematic of external KGW Raman laser and its Tm:YLF fundamental pump laser

A plano–plano mirror, AR coated at the fundamental wavelength and HR coated for 2170–2700 nm, is used as an input mirror for the Raman laser cavity, and a plano–concave mirror with a 200 mm ROC is used as an OC. This mirror has PR-coating of 90% reflectance between 2170 and 2700 nm and HR coating at the fundamental wavelength, enabling double-pass pumping of the 30 mm long KGW crystal, which is used as the active Raman medium. The crystal has AR coating for the fundamental and Raman wavelengths, and its cross-section is 7×7 mm^2. This crystal is oriented for propagation along the b-axis, having 901 cm^{-1} shift and 768 cm^{-1} shift, for E (electric field) perpendicular to the c-axis and a-axis, respectively [20]. As mentioned above, the control of the electric field polarization is facilitated using the HWP. The total Raman laser cavity length is 33 mm. The Raman beam waist diameter inside the KGW crystal is calculated by the ABCD matrix method to be 400 µm and 410 µm at 2197 nm and 2263 nm, respectively. The Raman laser beam has negligible divergence along the cavity. In order to improve the mode matching, a wider spot size of the pump laser was also

Optics EXPRESS

examined, but increasing the beam diameter gave lower power density, which led to slightly lower output energy from the Raman laser.

The pulse energy is measured by an energy meter (Ophir, PE50-C). Pulse temporal characterization is performed using an extended InGaAs fast photodetector with 200 ps rise-time (Alphalas, UPD-5N-IR2-P) and an oscilloscope (Agilent, DSO-X 2012A). The laser spectrum is acquired by a spectrometer (APE, Wavescan). Spatial profiling of the laser beam is performed using a pyroelectric camera (Pyrocam III-HR, Spiricon).

3. Results

The Raman laser output spectrum for each of the two Stokes shifts is shown in Fig. 2. Raman lasing at 2197 nm is observed for the 768 cm^{-1} shift, and emission at 2263 nm is observed for the 901 cm^{-1} shift. The two lines are observed for orthogonal orientations of the fundamental laser polarization to each other at the KGW crystal, as expected from the theory. Both output lines have spectral bandwidth of ~0.7 ± 0.2 nm FWHM.

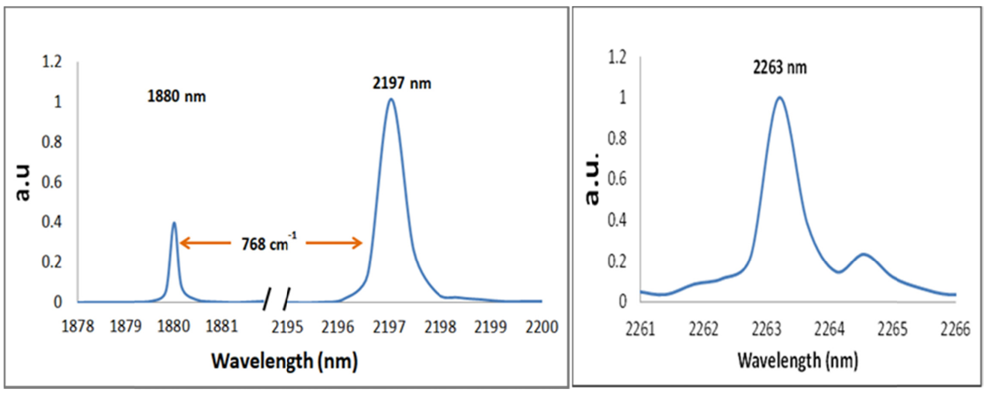

Fig. 2. Spectra of 768 cm^{-1} at 2197 nm and 901cm^{-1} at 2263 nm with fundamental wavelength at 1880 nm

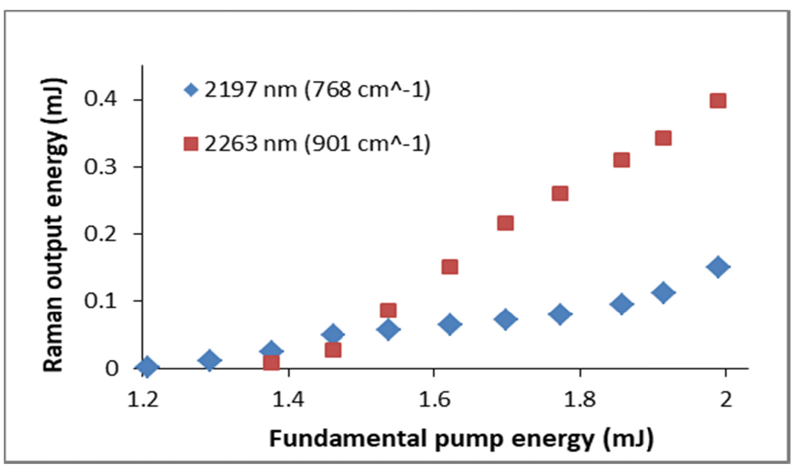

Fig. 3. Output energy of the Raman laser vs. fundamental laser energy

Optics EXPRESS

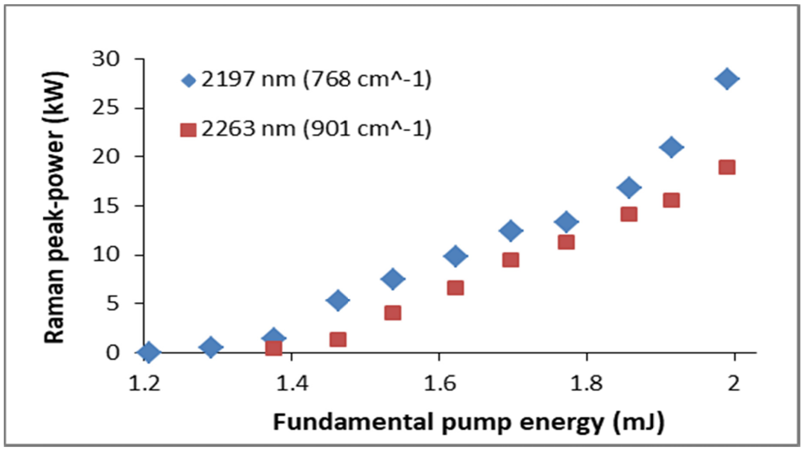

Fig. 4. Peak-power of the Raman laser vs. fundamental laser energy

Figure 3 and Fig. 4 present the output energy and peak power of the Raman laser, respectively, as functions of the pulse energy of the fundamental pump laser at a 1 kHz repetition rate. For the 2197 nm line, a threshold of 1.21 mJ/pulse from the fundamental laser is measured. At the highest available pump energy of 1.99 mJ/pulse, a maximum output energy of 0.15 mJ/pulse is attained, corresponding to a conversion efficiency of 7.5% and average power of 151 mW, having a slope efficiency of 16.7%. The duration of the 0.15 mJ output pulse is 5.4 ns FWHM, corresponding to a peak power of 27.8 kW.

For the 2263 nm line, the threshold from the fundamental laser is 1.38 mJ/pulse, whereas the maximal Raman output pulse energy is 0.4 mJ under an 1.99 mJ/pulse pump, corresponding to a conversion efficiency of 20% and an average power of 398 mW, having a slope efficiency of 66.7%. The pulse duration is measured to be 21 ns at FWHM, corresponding to a peak power of 19 kW. Temporal pulse measurements are shown in Fig. 5 for the 0.15 mJ, and the 0.4 mJ pulses, respectively. Pulse shortening related to the fundamental pulse duration of 34 ns is observed for both Raman lines.

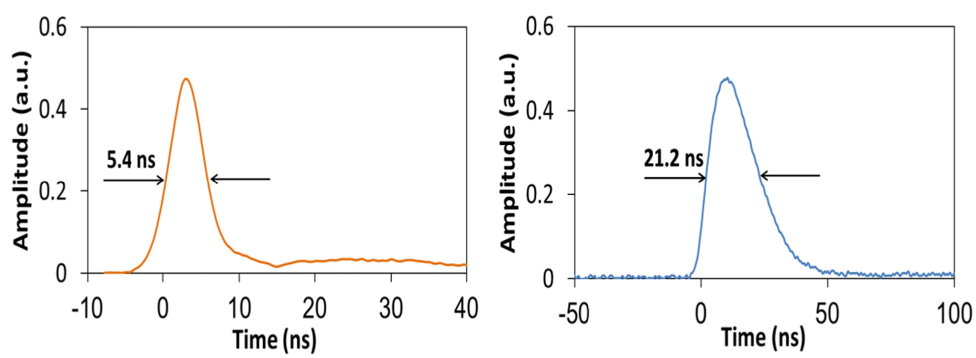

Fig. 5. Pulse duration of the 2197 nm line (left), and 2263 nm line (right)

Optics EXPRESS

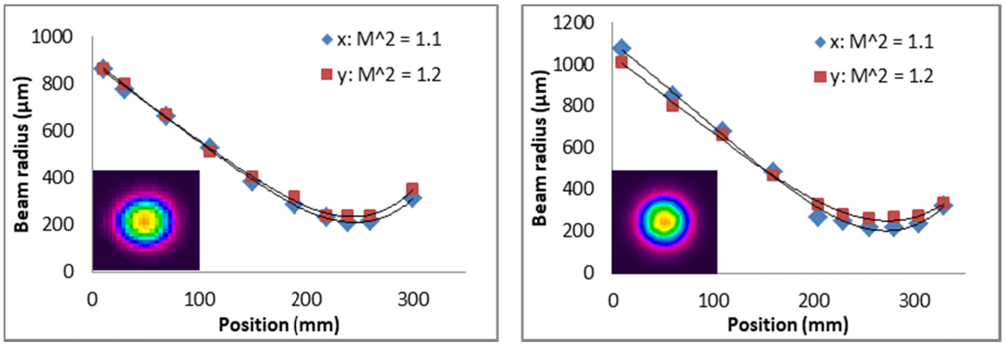

Fig. 6. M^2 measurement and beam profile for 2197 nm line (left), and 2263 nm line (right)

The M^2 of the pump and of the Stokes lines was measured along two orthogonal directions (called X and Y in Fig. 6.) by sampling the beam cross section at various planes across the beam caustic with a pyroelectric beam profiler. M^2 of 1.1 in the X direction and of 1.2 in the Y direction was measured for both Stokes lines, as shown in Fig. 6. relativly to M^2 of 1.4 (in both directions) for the fundamental pump source.

4. Discussion & conclusion

In this paper we demonstrated efficient Raman spectral shifting using the KGW. As mentioned above the Raman gain in the 2 µm regime is low compared to the Raman gain in the visible and 1 µm spectral range. For this reason, the $BaWO_4$, having higher gain coefficient in 1 µm, is often used as a Raman shifter. Nevertheless, for high-energy / high-power operation, the thermal properties and damage threshold of the crystal become important factors. Diamond, due to its superior thermal conductivity, is considered to be the best Raman gain material for such applications. However, diamond has high phonon energy, resulting in large Raman shift but also three phonon absorption band starting at 2.4 um, therefore, reducing the efficiency of Raman conversion at these wavelengths [28]. Besides, the diamond price is much higher than standard Raman crystals. Compared to other Raman crystals that are transparent in the 2-3 µm, the KGW has significantly higher damage threshold (e.g. 10 GW/cm^2, compared to 2 GW/cm^2 for $BaWO_4$ [29] and 1 GW/cm^2 for YVO_4 [6]). Also, its thermal lensing is considerably lower, owing to moderate negative thermo optic coefficient [6] which offsets the positive thermal lensing due to thermal expansion.

These advantages of KGW are important at longer wavelengths, due to the theoretically abovementioned dependence of the Raman gain coefficient on the wavelength, that requires higher pump density. Experimentally, this dependence is even faster than the theoretical inverse law with respect to pump wavelength. For example, in the 768 cm^{-1} line, the gain coefficient decreases from 11.8 cm/GW at 532 nm pump wavelength to 4.4 cm/GW at 1064 nm [6]. As far as we know, data for gain coefficients at longer pump wavelengths are not available. For the $BaWO_4$, for which the gain coefficient drops from 40 cm/GW to 8.5 cm/GW at the said wavelengths, this deviation from theory is even greater. To complete the comparison between the crystals, it is interest to calculate the gain coefficients at 1.9 µm for the KGW, and compare the outcome to a similar calculation result for the $BaWO_4$, and inspect if this trend continues at longer wavelengths.

Following Basiev [30], we can roughly to estimate the gain coefficient at this wavelength based on the experimental results presented in this paper. According to Basiev, the SRS threshold condition can be approximated by: $gI_{th}L_{eff} \sim 25$, where g is the effective Raman gain coefficient of the medium, I_{th} is the measured threshold intensity of the pump beam, and L_{eff} is the effective length of interaction between the pump beam and the Raman crystal. When the Raman medium is used inside a cavity configuration, the effective interaction

Optics EXPRESS

length is defined by: $L_{eff} = LN_{eff}$, where L is the crystal length and N_{eff} is the effective number of passes of SRS radiation trough the cavity. N_{eff} is given by:

$$N_{eff} \sim \left(\frac{L_r}{\tau_0 c} + \frac{1}{25} \ln\left(\frac{1}{\sqrt{R}} \right) \right)^{-1} \quad (1)$$

where L_r is the optical length of the cavity, c is the speed of light, τ_0 is the pump pulse duration, and R is the reflectance coefficient of the Raman cavity output coupler.

Based on the measured parameters of 34 ns pump pulse duration, 90% output coupler reflectivity at the first Stokes wavelength, and a cavity optical length of ~6 cm, the effective number of passes of the SRS radiation trough the cavity is estimated to be ~120 passes. This number translates to an effective interaction length of ~360 cm for a 3 cm Raman crystal. For this calculation, we took the average value of the pump beam diameter in the cavity (260 µm)

From these numbers, given the measured intensity thresholds for the two crystal directions, the Raman gain coefficient of KGW at 1.9 µm can be given a lower bound of 1 cm/GW for the 786 cm^{-1} mode, and 0.9 cm/GW for the 901 cm^{-1} mode. We should emphasize that this is only a first order approximation, and should be refined by further measurements. Moreover, it should be pointed out that, according to Reference [31,32], the estimated coefficient presented here is an effective Raman gain coefficient and not the material gain coefficient of the medium, due to the gain reduction factor arising from the spatial and spectral mismatch between the pump beam and stokes beam.

Similar calculation, relying on the same method, for the $BaWO_4$, yielded a gain coefficient of 1.1 cm/GW for slightly longer wavelength of 1.94 µm [19]. These values show that the gain difference between the KGW and the more popular $BaWO_4$ becomes less significant in the SWIR region. Moreover, the superior damage threshold of KGW confers to this medium an important advantage in power scaling.

Another important insight from the results that should be discussed is the lower threshold observed at the 2197 nm line compared to the 2263nm line. This is in accordance with the higher gain coefficient of the 768 cm^{-1} shift compared to the 901 cm^{-1} shift reported for 1064 nm [6]. The results presented here support this ratio between the two lines also for this spectral range. However, despite the lower threshold for the 2197 nm line, the 2263 nm line exhibits higher output energy at maximal pump pulse energy. An additional noticeable difference is the pulse duration measured for the 2197 nm line which is much shorter than that measured for the 2263 nm line. These two observations may suggest that for the 2197 nm line a 2nd Stokes conversion builds up inside the cavity, and decreases the output level of the first Stokes. The 2nd Stokes wavelength is 2643 nm which is inside the OC reflectivity range, hence can be sustained by the SRS process. Note that this wavelength is partially absorbed by the fused silica substrate of the OC, hence attenuated by ~40%. Contrarily, for the other Stokes line at 2263 nm the 2nd Stokes is at ~2840 nm which is not reflected by the OC, hence all the available Raman gain is channeled into the 1st Stokes. This may explains why the 2263 nm line is stronger than the 2197 nm line. This assumption should be confirmed with advanced spectral measurements in future work.

Unfortunately, due to technical difficulties and limitations on setup and measurement devices, the 2nd Stokes was not observed and measured. However, to demonstrate the effect of pulse shortening due to 2nd Stokes generation a numerical simulation was run. In the simulation the Raman intensity coupled propagation equations [33] of the pump, 1st and 2nd Stokes are solved. The Gaussian temporal shaped pump pulse is divided into short time slices, each one equals to double pass duration in the cavity. For each time slice the differential equations are integrated, taking into account cavity boundary conditions, where the results of previous time slice integration serve as an initial condition. The simulation doesn't take into account transverse effects such as diffraction and modes overlap between pump and Stokes beams, as well as time derivative of the pump and Stokes fields. Accordingly, it does not purport to accurately predict the experimental results but to show phenomenologically the effect of pulse shortening. In order to simulate a case close to the experiment, the pump and Stokes wavelengths, crystal length and mirrors reflectivity were adapted to the experimental setup. For the Raman gain coefficient g = 1cm/GW was used, and ω = 120 μm was used for the beams waists. Figure 7 presents temporal results for 2 mJ of pump energy for the case of OC with R = 0 at the 2nd Stokes and for the case of R = 90% at the 2nd Stokes. As can be seen in the figure, when mirror reflection set to R = 0 at 2nd Stokes wavelength there is no output power at 2nd Stokes and the 1st Stokes pulse duration is ~20 ns. However, at the case of R = 0.9 for the 2nd Stokes an additional output pulse appears accompanied by 1st Stokes pulse shortening down to ~6 ns. Pulse shortening due to 2nd Stokes generation was also presented experimentally as well as numerically by Sabella et al. [10].

In terms of output energy, the simulation predicts ~1.25 mJ and ~1.45 mJ threshold energy where using g = 1.2 cm/GW and g = 1 cm/GW, for the 768 cm^{-1} and 901 cm^{-1}, respectively. These values fairly agree with the experimental threshold results. Regarding the output energy curves, the simulation predicts higher slope efficiencies then the experimental results, and shows lower output energy at the 1st Stokes where R = 90% for the Second Stokes.

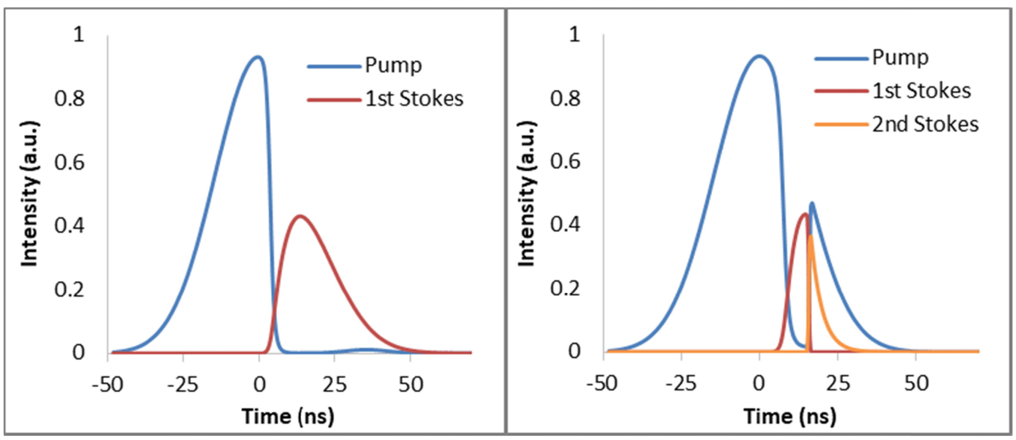

Fig. 7. Simulation of the pulse duration for negligible (left) and 90% (right) mirror reflectivity at the 2nd Stokes

In conclusion, in this paper, an efficient laser for SRS wavelength conversion in the 2 μm region using an external cavity configuration is presented. A KGW active medium pumped by an 1880 nm actively Q-switched Tm:YLF laser displays spectral shifting of two distinct output wavelengths at 2197 nm and 2263 nm. . The external-cavity architecture, unlike intra cavity configuration, doesn't limit the design of the pump laser, allowing achieving both high energy and good performance for the Tm-doped laser, as well as leveraging the good optical and thermal properties of the KGW crystal for efficient wavelength conversion. The laser exhibits the highest energy of 0.4 mJ/pulse yet reported at the 2 μm spectral regime for Raman conversion at the first stokes wavelength. These results allow to evaluate a lower bound for the Raman gain coefficient for KGW at 1.9 μm. To the best of our knowledge, this is the first implementation of a solid-state Raman laser based on a KGW crystal as a gain medium in the 2 μm region, showing that KGW is suitable for efficient SRS conversion in this spectral range for its two shifts, with performance comparable to other Raman crystals. Added to its optical, mechanical and thermal properties, and based on the comprehensive use of this crystal at shorter wavelengths, it appears to be a good candidate for Raman lasers in the 2 μm segment.

Acknowledgments

U. Sheintop would like to thank E. Perez and R. Nahear for the fruitful discussions and collaboration.

References

1. V. Serebryakov, É. Boĭko, A. Kalintsev, A. Kornev, A. Narivonchik, and A. Pavlova, "Mid-IR laser for high-precision surgery," J. Opt. Technol. **82**(12), 781 (2015).
2. I. Mingareev, F. Weirauch, A. Olowinsky, L. Shah, P. Kadwani, and M. Richardson, "Welding of polymers using a 2 μm thulium fiber laser," Opt. Laser Technol. **44**(7), 2095–2099 (2012).
3. A. Godard, "Infrared (2-12 μm) solid-state laser sources: a review," C. R. Phys. **8**(10), 1100–1128 (2007).
4. I. Sorokina and K. Vodopyanov, *Solid-State Mid-Infrared Laser Sources* (Springer, 2003).
5. K. Scholle, P. Fuhrberg, P. Koopmann, and S. Lamrini, *2 μm Laser Sources and Their Possible Applications* (INTECH Open Access Publisher, 2010).
6. J. A. Piper and H. M. Pask, "Crystalline Raman Lasers," IEEE J. Sel. Top. Quantum Electron. **13**(3), 692–704 (2007).
7. P. Cerný, H. Jelinkova, P. G. Zverev, and T. T. Basiev, "Solid state lasers with Raman frequency conversion," Prog. Quantum Electron. **28**(2), 113–143 (2004).
8. H. M. Pask, "The design and operation of solid-state Raman lasers," Prog. Quantum Electron. **27**(1), 3–56 (2003).
9. T. T.. Basiev and R. C. Powell, *Handbook of Laser Technologies & Applications B1.7* (CRC Press, 2003), pp. 1–29.
10. A. Sabella, J. A. Piper, and R. P. Mildren, "Efficient conversion of a 1.064 μm Nd:YAG laser to the eye-safe region using a diamond Raman laser," Opt. Express **19**(23), 23554–23560 (2011).
11. X. Duan, Y. Ding, B. Yao, and Y. Wang, "High power acousto-optical Q-switched Tm:YLF-pumped Ho:$GdVO_4$ laser," Optik (Stuttg.) **163**, 39–42 (2018).
12. B. Cole and L. Goldberg, "Highly efficient passively Q-switched Tm:YAP laser using a Cr:ZnS saturable absorber," Opt. Lett. **42**(12), 2259–2262 (2017).
13. A. Korenfeld, D. Sebbag, U. Ben-Ami, E. Shalom, G. Marcus, and S. Noach, "High pulse energy passive Q-switching of a diode-pumped Tm:YLF laser by Cr:ZnSe," Laser Phys. Lett. **12**(4), 045804 (2015).
14. D. Sebbag, A. Korenfeld, U. Ben-Ami, D. Elooz, E. Shalom, and S. Noach, "Diode end-pumped passively Q-switched Tm:YAP laser with 1.85-mJ pulse energy," Opt. Lett. **40**(7), 1250–1253 (2015).
15. V. G. Savitski, "Experimental analysis of emission linewidth narrowing in a pulsed $KGd(WO_4)_2$ Raman laser," Opt. Express **22**(18), 21767–21774 (2014).
16. D. Spence, "Spectral effects of stimulated Raman scattering in crystals," Prog. Quantum Electron. **51**, 1–45 (2017).
17. T. Basiev, M. Basieva, M. Doroshenko, V. Fedorov, V. Osiko, and S. Mirov, "Stimulated Raman scattering in mid IR spectral range 2.31–2.75–3.7 μm in $BaWO_4$ crystal under 1.9 and 1.56 μm pumping," Laser Phys. Lett. **3**(1), 17–20 (2006).
18. L. Batay, A. Kuzmin, A. Grabtchikov, V. Lisinetskii, V. Orlovich, A. Demidovich, A. Titov, V. Badikov, S. Sheina, V. Panyutin, M. Mond, and S. Kück, "Efficient diode-pumped passively Q-switched laser operation around 1.9 μm and self-frequency Raman conversion of Tm-doped $KY(WO_4)_2$," Appl. Phys. Lett. **81**(16), 2926–2928 (2002).
19. J. Zhao, Y. Li, S. Zhang, L. Li, and X. Zhang, "Diode-pumped actively Q-switched Tm:YAP/$BaWO_{(4)}$ intracavity Raman laser," Opt. Express **23**(8), 10075–10080 (2015).
20. P. Cheng, J. Zhao, F. Xu, X. Zhou, and G. Wang, "Diode-pumped mid-infrared YVO_4 Raman laser at 2418 nm," Appl. Phys. B **124**, 5 (2017).
21. J. Zhao, X. Zhang, X. Guo, X. Bao, L. Li, and J. Cui, "Diode-pumped actively Q-switched Tm, Ho:$GdVO_4$/$BaWO_4$ intracavity Raman laser at 2533 nm," Opt. Lett. **38**(8), 1206–1208 (2013).
22. X. Zhang, Y. Ding, Y. Qiao, G. Li, and J. Cui, "Diode-end-pumped efficient 2533 nm intracavity Raman laser with high peak power," Opt. Commun. **355**, 433–437 (2015).
23. O. Kuzucu, "Watt-level, mid-infrared output from a $BaWO_4$ external-cavity Raman laser at 2.6 μm," Opt. Lett. **40**(21), 5078–5081 (2015).
24. A. Sabella, J. A. Piper, and R. P. Mildren, "Diamond Raman laser with continuously tunable output from 3.38 to 3.80 μm," Opt. Lett. **39**(13), 4037–4040 (2014).
25. I. V. Mochalov, "Laser and nonlinear properties of the potassium gadolinium tungstate laser crystal $KGd(WO_4)_2$:Nd^{3+}-(KGW:Nd)," Opt. Eng. **36**, 1660–1669 (1997).
26. U. Sheintop, D. Sebbag, and S. Noach, "Diode End Pump External KGW/ Tm:YLF Raman Laser," *Advanced Solid State Laser Congress 2018 (ASSL)* (Optical Society of America, 2018).
27. U. Sheintop, E. Perez, D. Sebbag, P. Komm, G. Marcus, and S. Noach, "Actively Q-switched tunable narrow bandwidth milli-Joule level Tm:YLF laser," Opt. Express **26**(17), 22135–22143 (2018).
28. A. Zaitsev, *Optical Properties of Diamond* (Springer, 2010), pp. 23–27.
29. http://eksmaoptics.com/nonlinear-and-laser-crystals/crystals-for-stimulated-raman-scattering/barium-and-strontium-tungstate-molybdate-crystals-for-raman-shift/

30. T. Basiev, M. Basieva, A. Gavrilov, M. Ershkov, L. Ivleva, V. Osiko, S. Smetanin, and A. Fedin, “Efficient conversion of Nd:YAG laser radiation to the eye-safe spectral region by stimulated Raman scattering in $BaWO_4$ crystal,” Quantum Electron. **40**(8), 710–715 (2010).
31. D. Parrotta, A. Kemp, M. Dawson, and J. Hastie, “Multiwatt, Continuous-Wave, Tunable Diamond Raman Laser With Intracavity Frequency-Doubling to the Visible Region,” IEEE J. Sel. Top. Quantum Electron. **19**(4), 1400108 (2013).
32. J. Lin, H. M. Pask, A. J. Lee, and D. J. Spence, “Study of relaxation oscillations in continuous-wave intracavity Raman lasers,” Opt. Express **18**(11), 11530–11536 (2010).
33. S. Ding, X. Zhang, Q. Wang, P. Jia, C. Zhang, and B. Liu, “Numerical optimization of the extracavity Raman laser with barium nitrate crystal,” Opt. Commun. **267**(2), 480–486 (2006).